



Geiger-Mode Avalanche Photodiodes for Near-Infrared Photon Counting

Mark Itzler

Princeton Lightwave Inc., Cranbury, NJ USA

Co-authors and Collaborators

PLI CO-AUTHORS: Xudong Jiang, Rafael Ben-Michael, Krystyna Slomkowski

COLLABORATORS for device characterization:

Bruce Nyman.....*PLI*

Mark Entwistle

Mike Krainak.....*NASA/GSFC*

Stewart Wu

Xiaoli Sun

Sergio Cova.....*Politecnico di Milano*

Alberto Tosi

Franco Zappa

Radu Ispasoiu.....*Credence Systems*

Gary Smith.....*MIT Lincoln Laboratories*

Gerald Buller.....*Heriot-Watt University*

Sara Pelligrini

Presentation outline

- **Motivation for single photon detectors**
- **Overview of Geiger-mode avalanche photodiodes**
- **Geiger-mode operation**
- **Present performance and challenges**
 - **Dark count rate**
 - **Afterpulsing effects**
- **Conclusions**

Motivation for single photon detectors

Examples of photon counting applications for $\lambda > 1.0 - 1.7 \mu\text{m}$:

➤ **Communications**

- Secure communications (e.g., quantum key distribution)
- Free space optical communication in photon-starved applications

➤ **Remote sensing**

- 3-D Imaging
- Lidar / atmospheric sensing

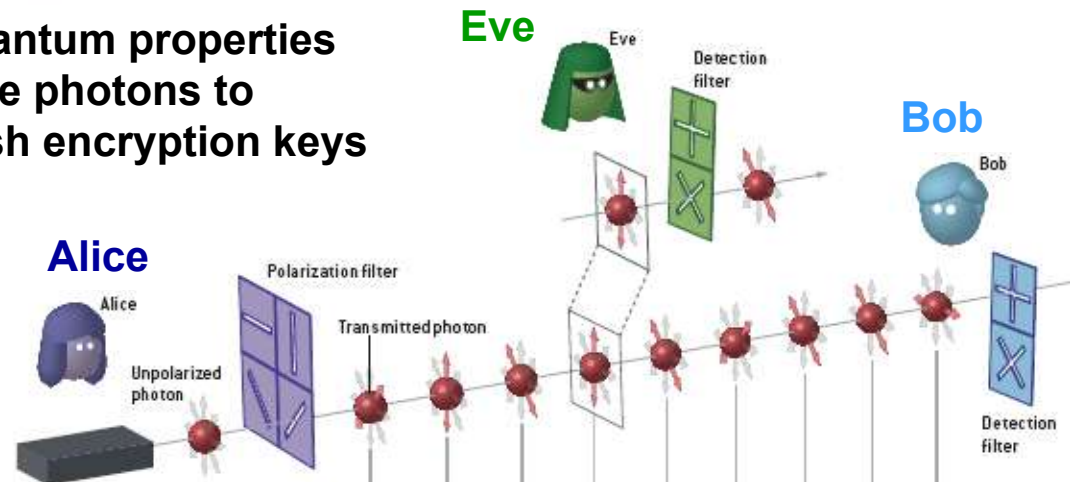
➤ **Industrial and Biomedical**

- Semiconductor diagnostics
- Single photon fluorescence (e.g., quantum dot markers)

SPC Application: Next-gen Communications

➤ Secure Communications through Quantum Key Distribution

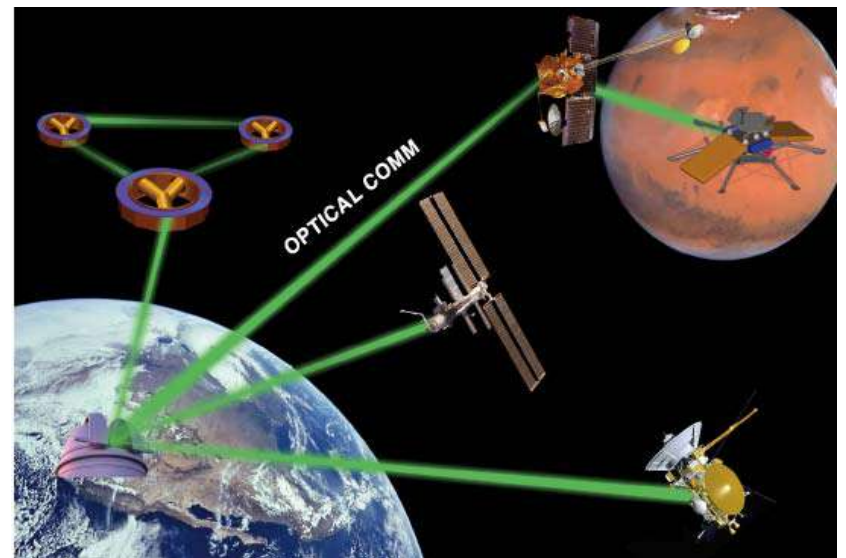
- Use quantum properties of single photons to establish encryption keys



➤ Long-range Free Space Communications

- Single photon sensitivity for photon-starved communication links
- “N bits per photon” protocols

JPL Optical
Communications Group –
vision of free space comm



SPC Application: 3-D Imaging

- **Perform ladar (“laser radar”) measurement at every pixel of array**
 - Obtain time-of-flight information at every pixel to calculate “depth”
 - Allows imaging through obscuring elements (e.g., foliage, netting, etc.)

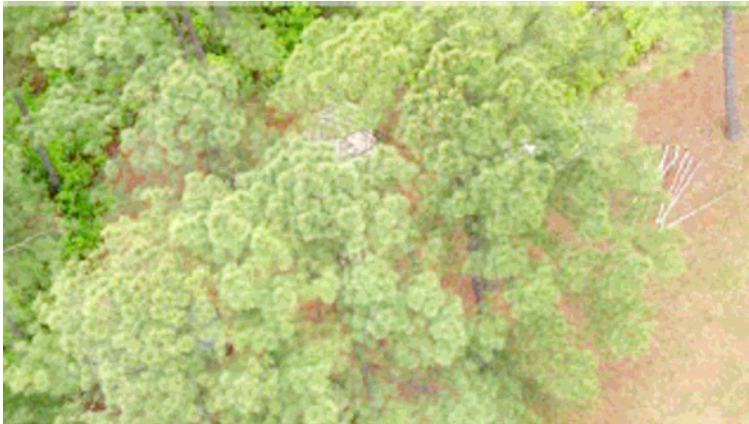
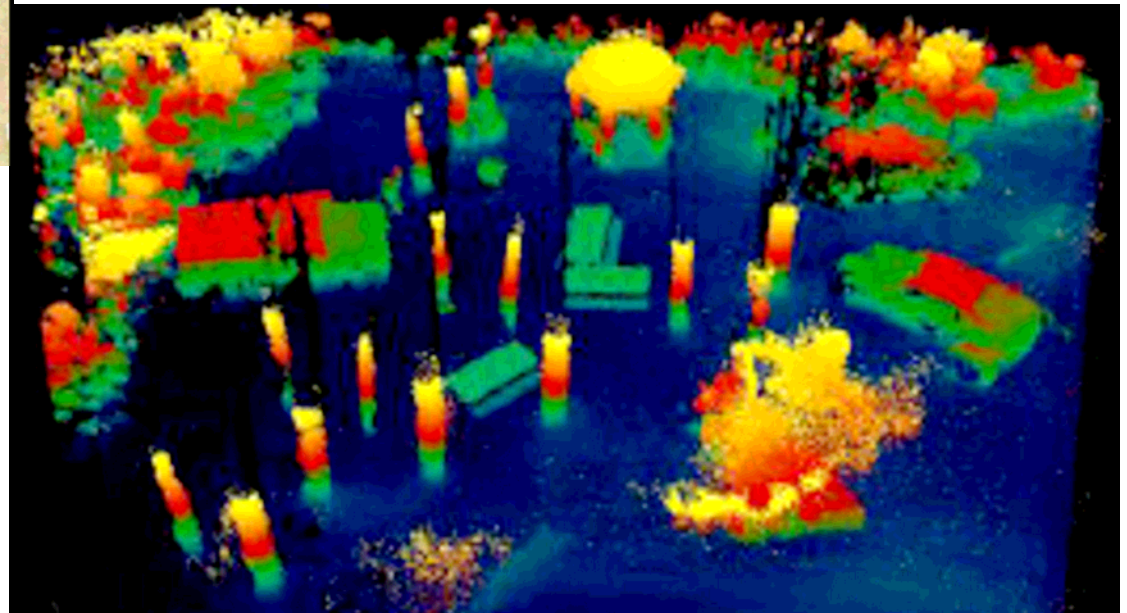


Image of scene beneath foliage (e.g., vehicles, picnic tables)

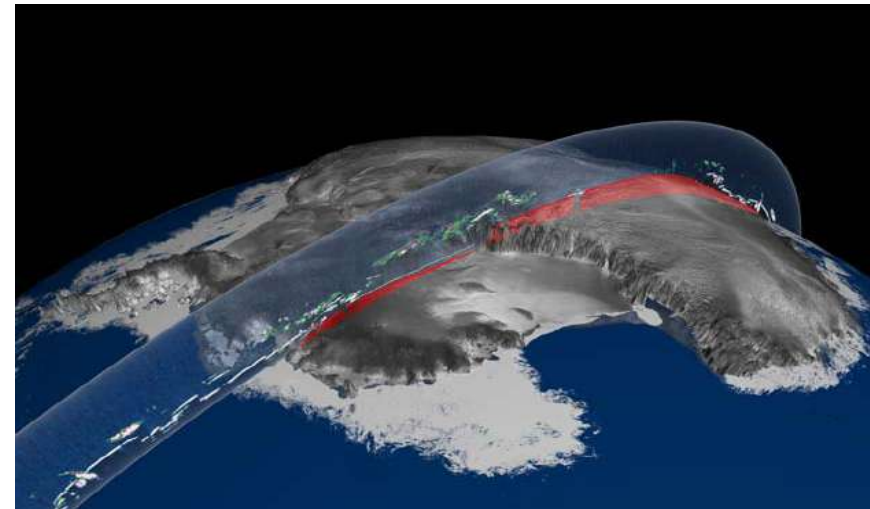


B. Aull, et al., SPIE 5353,
p. 105 (2004)

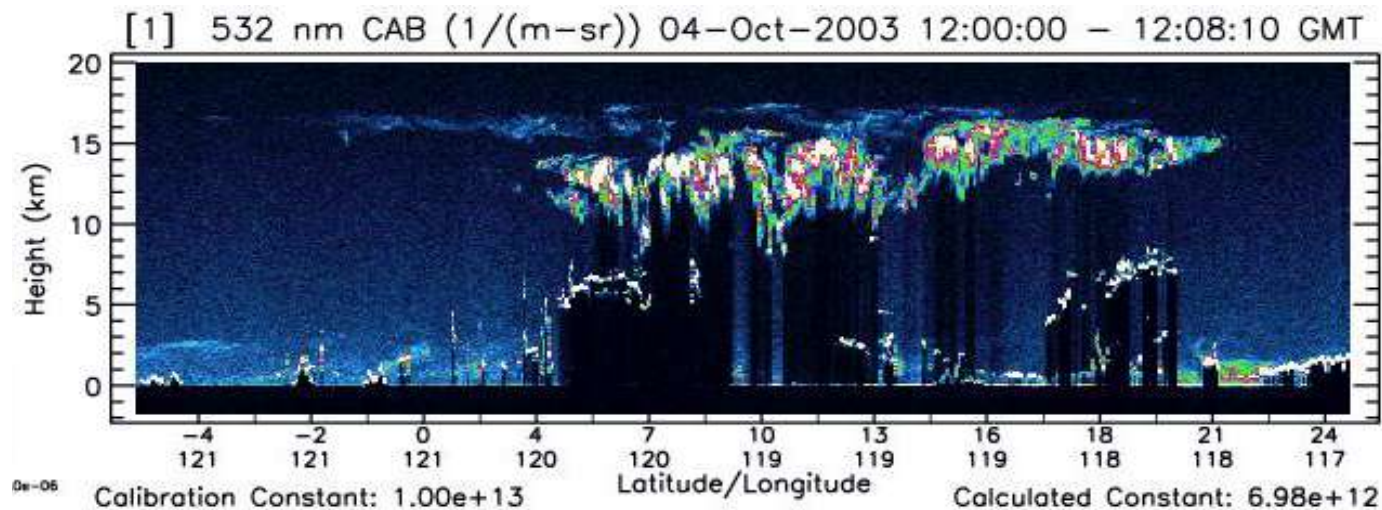
SPC Application: Atmospheric Lidar

➤ NASA ICESat/GLAS

Ice, Cloud, and land Elevation Satellite
on the
Geoscience Laser Altimeter System

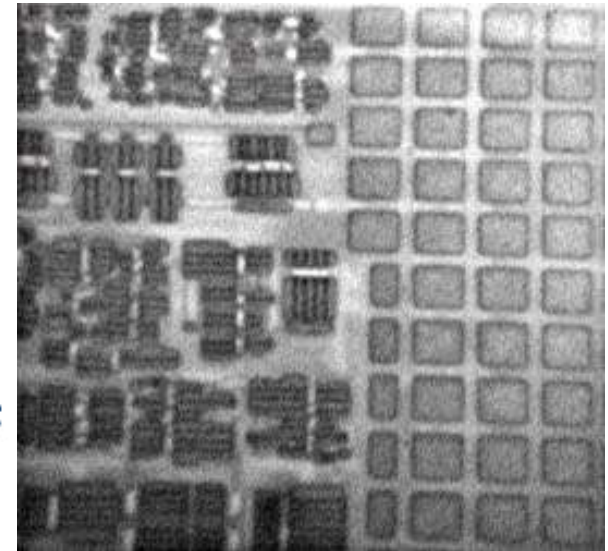


Atmospheric mapping by lidar along Earth's circumference

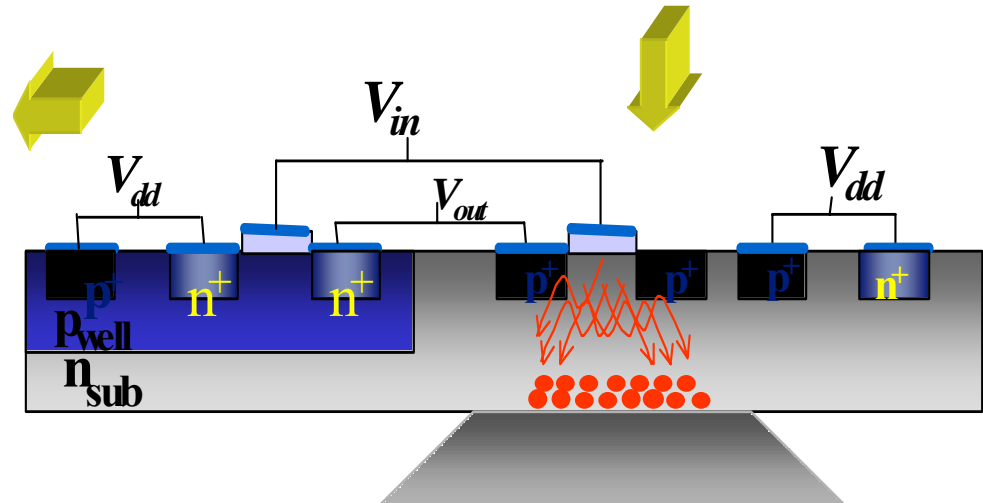
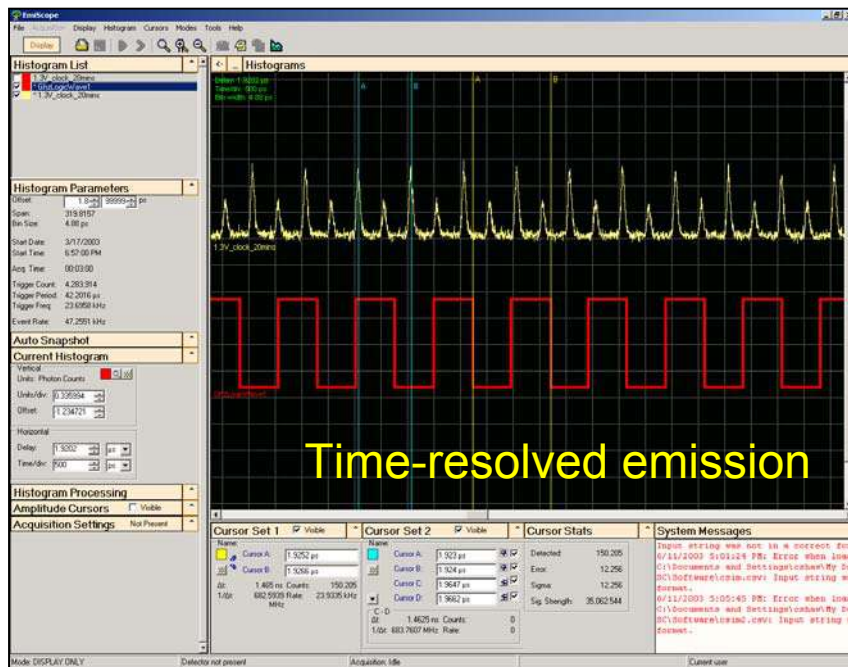


SPC Application: Semiconductor diagnostics

- Time-resolved photon counting to measure CMOS hot carrier luminescence
 - circuit design and debugging
 - circuit failure analysis



credence



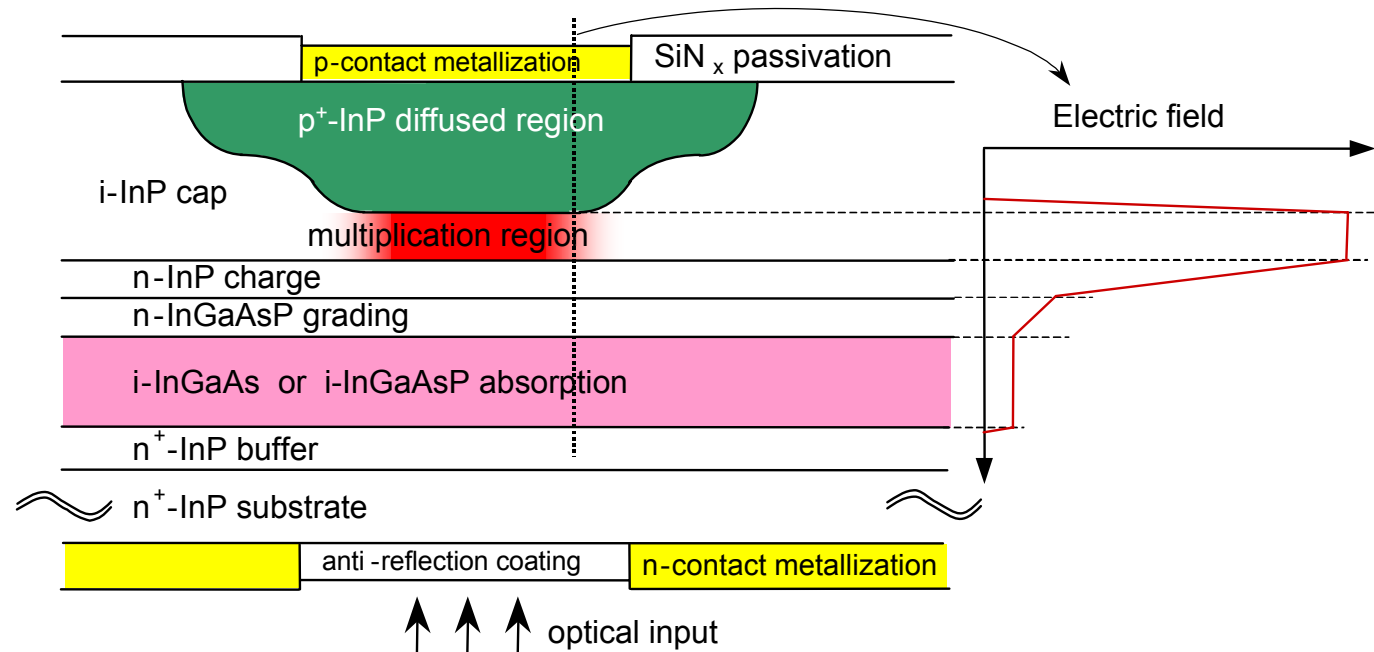
Collection (optics & detector)

Presentation outline

- Motivation for single photon detectors
- **Overview of avalanche photodiode structure**
- Geiger-mode operation
- Present performance and challenges
 - Dark count rate
 - Afterpulsing effects
- Conclusions

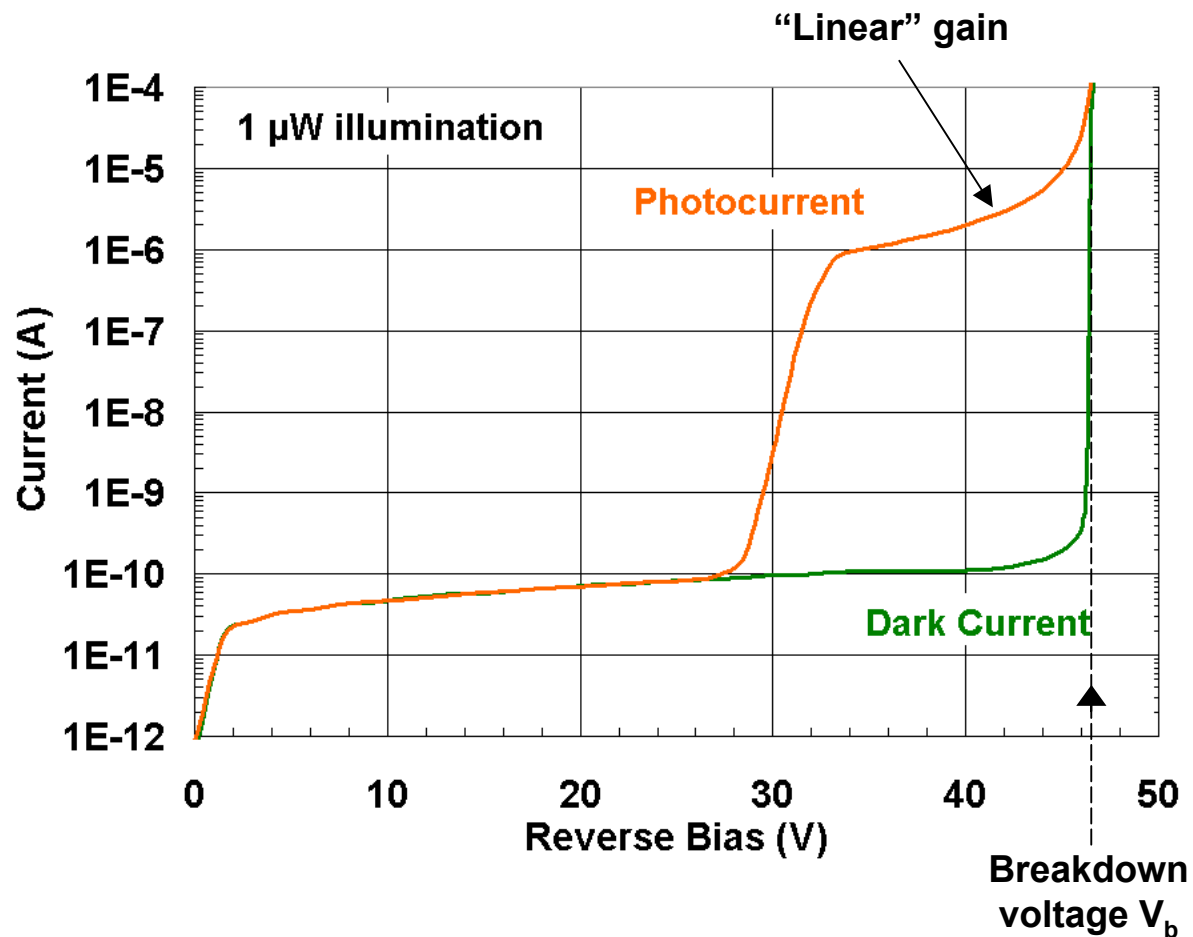
InGaAsP/InP avalanche diode design platform

- **Separate Absorption, Charge, and Multiplication (SACM) structure**
 - High E-field in multiplication region → induce avalanching
 - Low E-field in absorption region → suppress tunneling
- **Planar passivated, dopant diffused device structure**
 - Stable and reliable buried p-n junction
 - Widespread deployment of device platform in telecom Rx



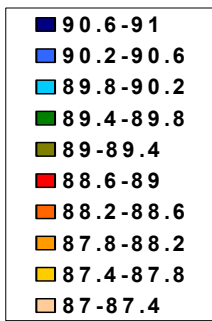
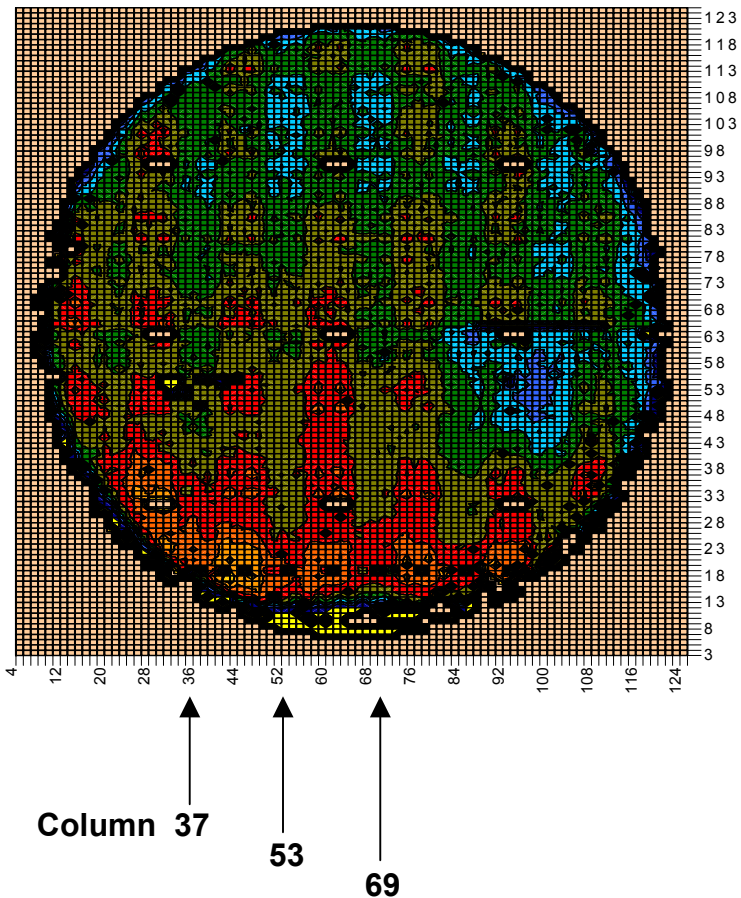
APD Current-Voltage Characteristics

- Linear mode performance is behavior below breakdown voltage V_b
 - Output photocurrent below V_b is linearly proportional to input optical power

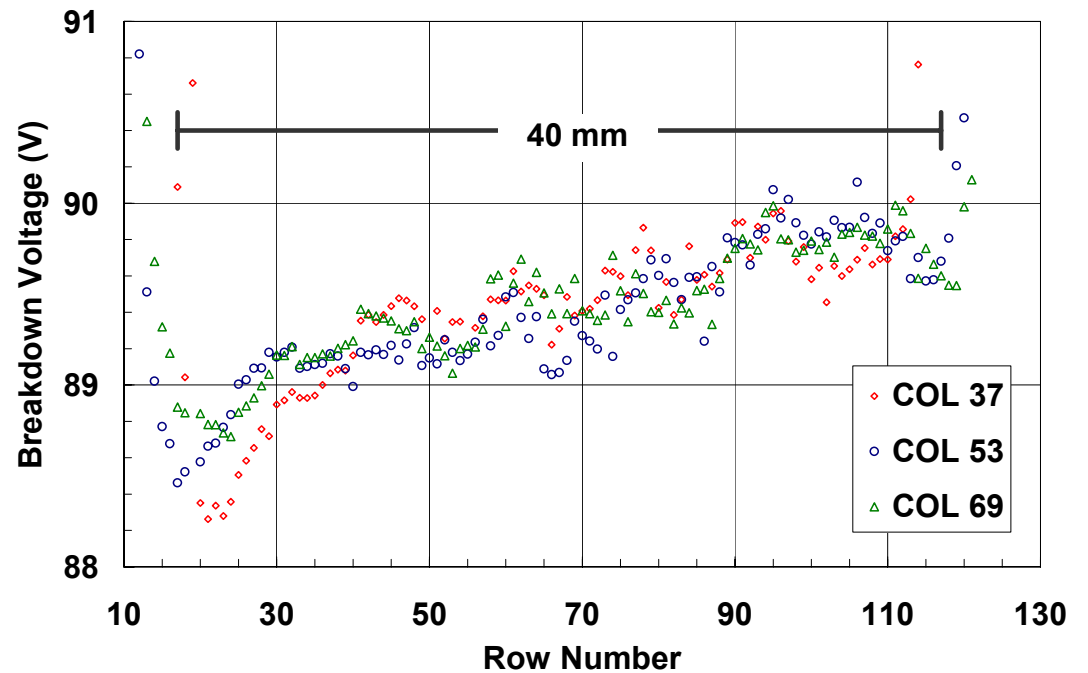


Performance uniformity at wafer level

- Breakdown voltage is very sensitive to structural details
 - Provides good measure for consistency of many device attributes



- Ex.: 1.06 μm SPAD wafer
 - Intentional systematic variation to confirm diffusion control process
- V_b variation: $\sim 0.03 \text{ V per mm}$



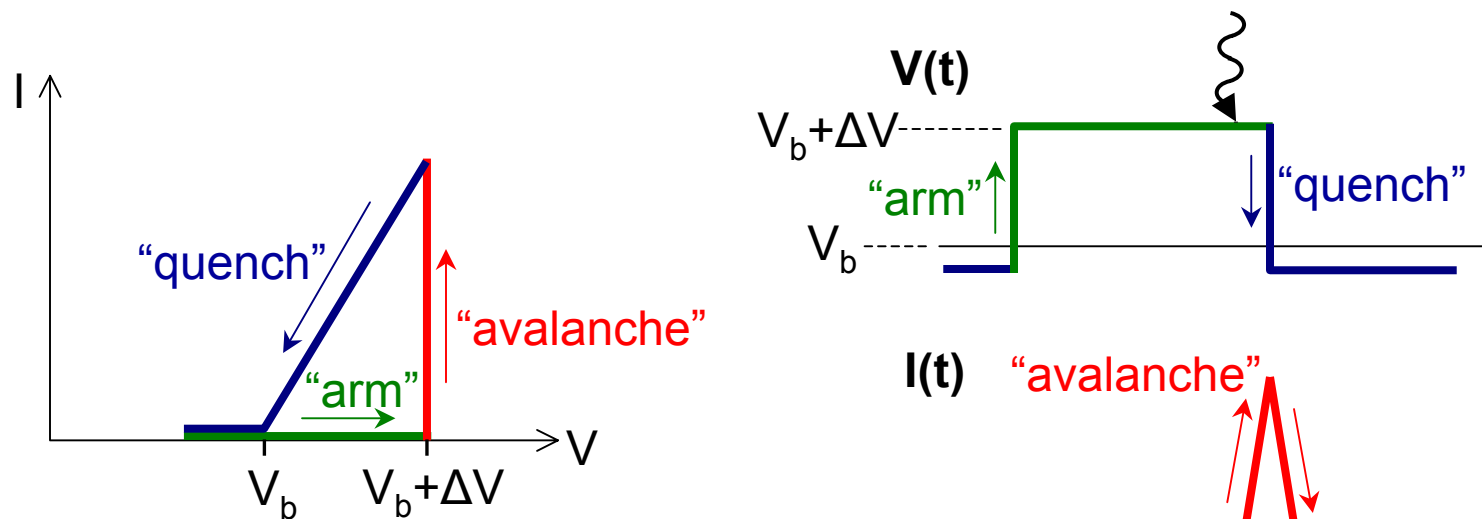
Presentation outline

- Motivation for single photon detectors
- Overview of Geiger-mode avalanche photodiodes
- **Geiger-mode operation**
- Present performance and challenges
 - Dark count rate
 - Afterpulsing effects
- Conclusions

Geiger mode operation

➤ Single photon avalanche diodes (SPADs) operate in “Geiger mode”

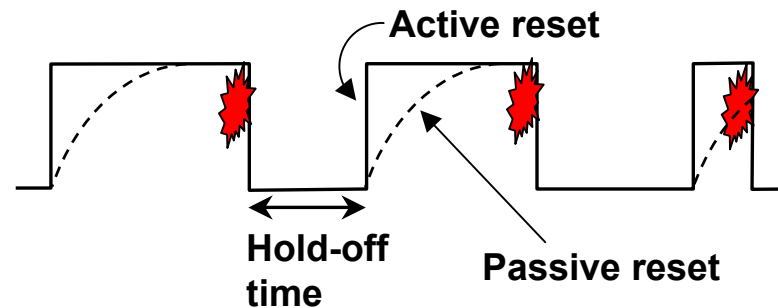
- Bias above breakdown voltage V_b by overbias ΔV
- Single photon induces avalanche leading to macroscopic current pulse
 - Avalanche detected using threshold detection circuit
- Used as a photon-activated switch with purely digital output
- Avalanche must be quenched after detection by lowering bias below V_b



Geiger mode quenching schemes

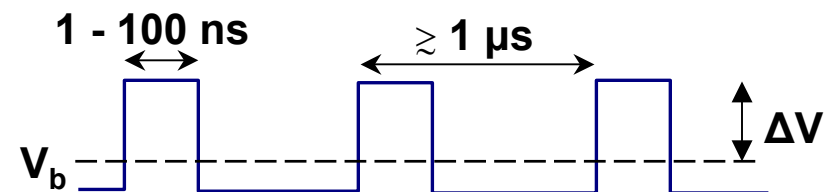
➤ Free-running operation

- SPAD is “armed” (biased above breakdown) until avalanche occurs



➤ Gated-mode operation

- Most relevant operation for InP-based SPADs
- Periodic arming and disarming of the SPAD



- Short gates (~ 1 ns) are ideal if photon arrival is deterministic (e.g., communications)

SPAD performance parameters

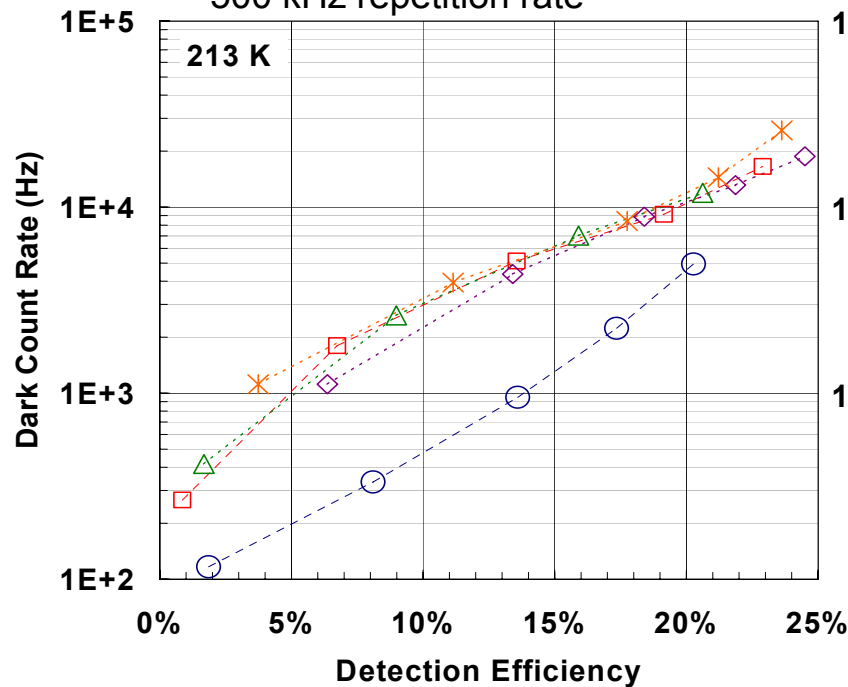
- **Detection efficiency (DE):** probability of detecting incident photon
- **Dark count rate (DCR):** probability of “false” detection (no incident photon)
- **Afterpulsing (AP):** increase in dark count rate following previous detection
 - Mitigated only by limiting repetition rate
- **Timing jitter (TJ):** randomness in detection timing
- **Important performance trade-offs to be managed**
 - Increase overbias: **DE** 😊 , **TJ** 😊 , **DCR** 😞
 - Decrease temperature: **DCR** 😊 , **AP** 😞

DCR vs. DE trade-off

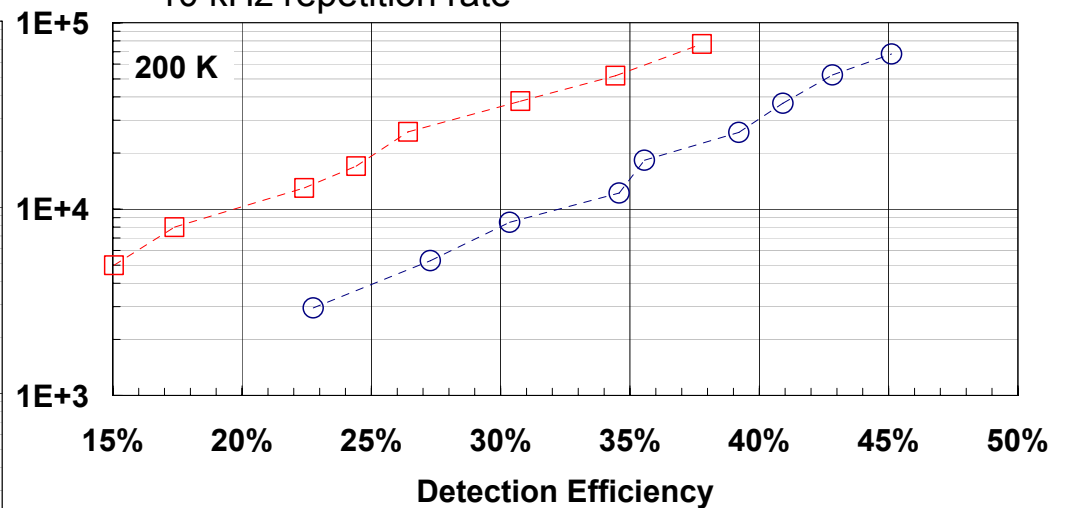
- Most important SPAD performance tradeoff: DCR vs. DE
- Typical performance: 10 kHz DCR at 20% DE, 100 kHz at 40% DE

Data for 25 μm diameter InGaAs/InP SPADs for 1.5 μm

- 1 ns gating
- 500 kHz repetition rate



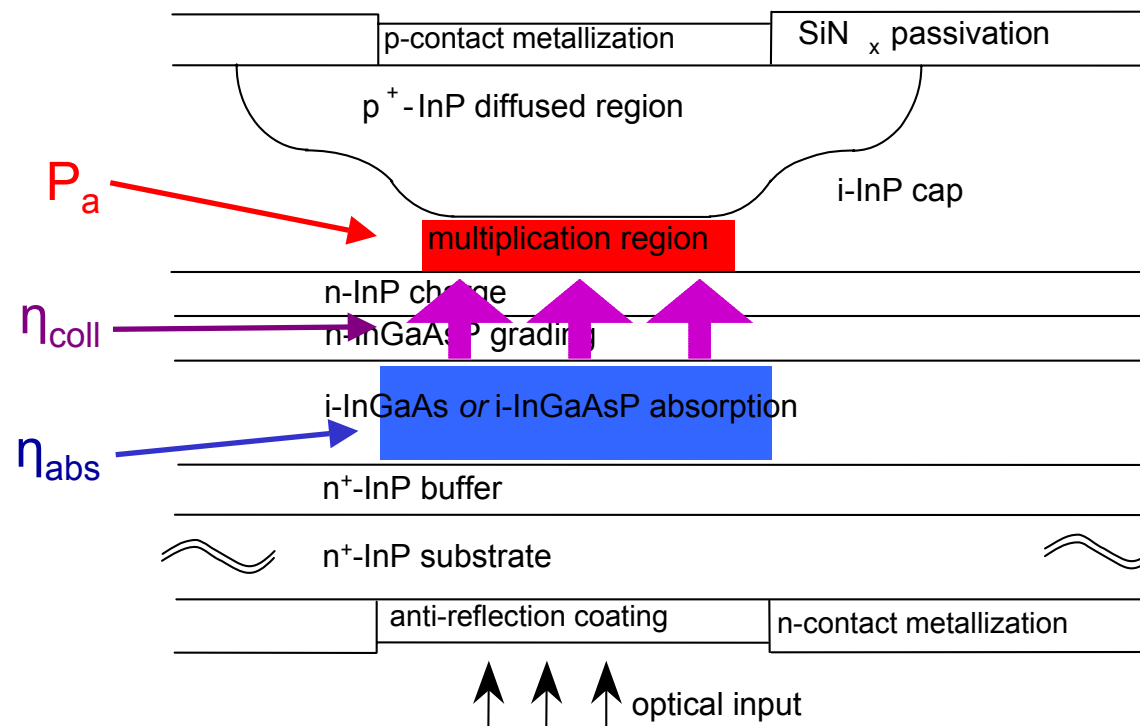
- 200 ns gating with active quenching
- 10 kHz repetition rate



--○-- "hero" devices

Photon Detection Efficiency

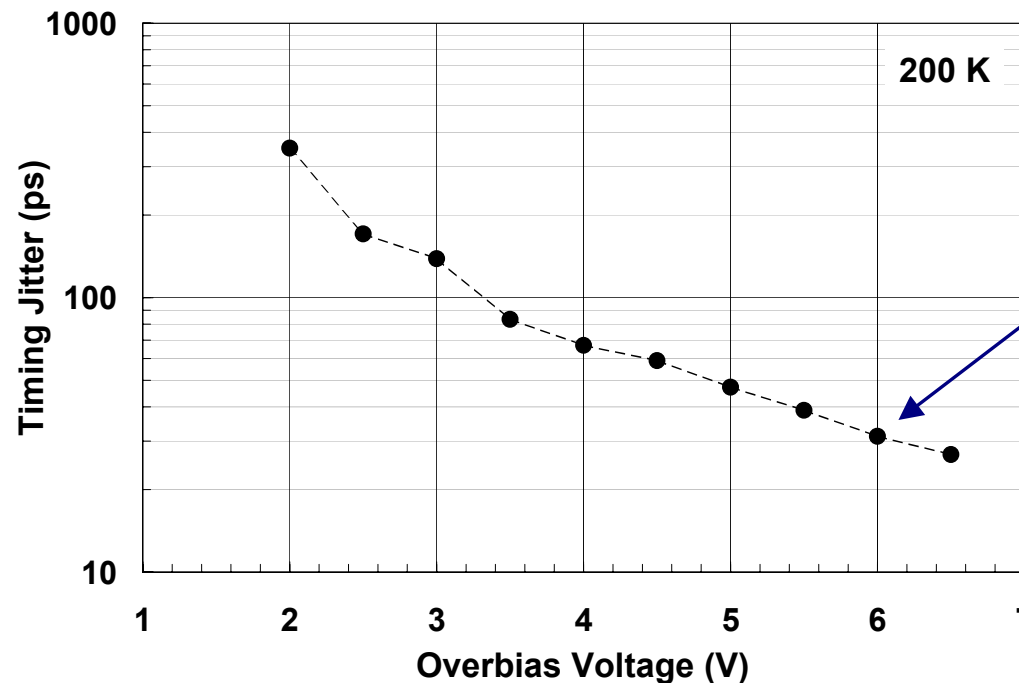
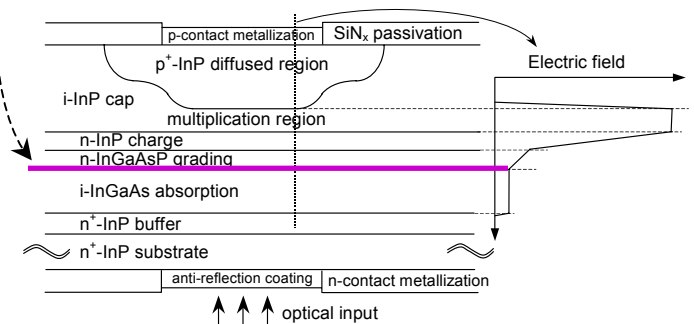
- **Detection efficiency: $DE = \eta_{\text{abs}} \times \eta_{\text{coll}} \times P_a$**
- η_{abs} : probability of photon absorption (i.e., quantum efficiency)
 - η_{coll} : probability of carrier injection to multiplication region
 - P_a : probability that injected carrier initiates self-sustaining avalanche



Timing Jitter

- Factors contributing to timing jitter:
 - Absorption location (through varying transit time)
 - **Carrier propagation delay at interfaces**
 - Avalanche build-up time (vertical and lateral)
- SPAD capability generally < 100 ps
 - Electronics design is critical to TJ performance

Critical interface for primary hole trapping



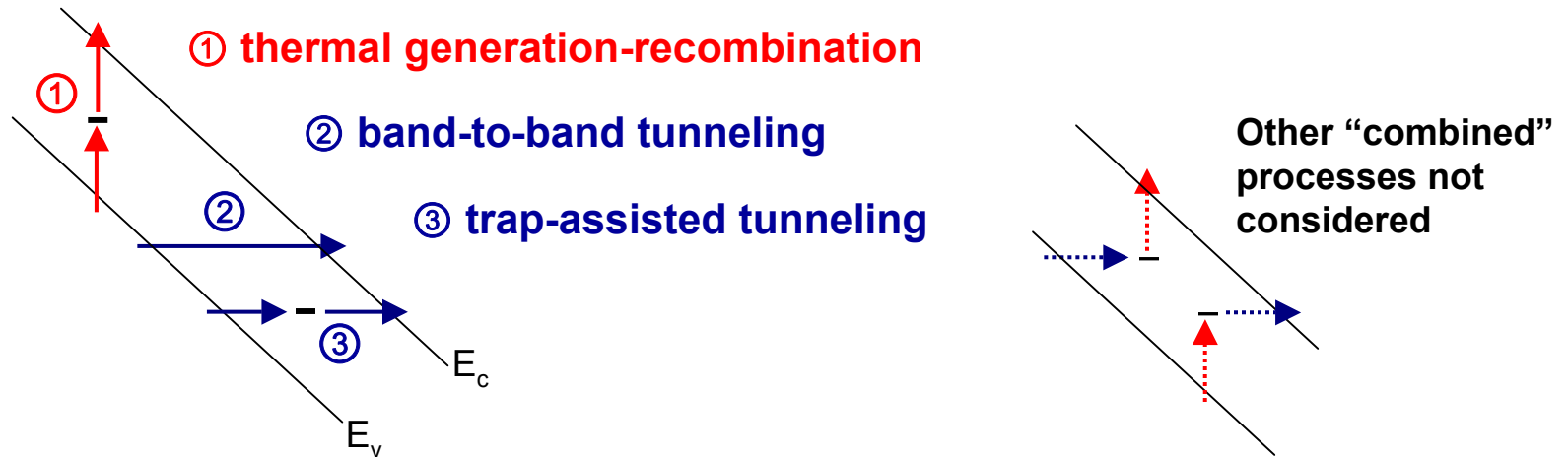
30 ps at $\Delta V = 6$ V

Presentation outline

- Motivation for single photon detectors
- Overview of Geiger-mode avalanche photodiodes
- Geiger-mode operation
- Present performance and challenges
 - **Dark count rate**
 - Afterpulsing effects
- Conclusions

Dark count rate behavior and mechanisms

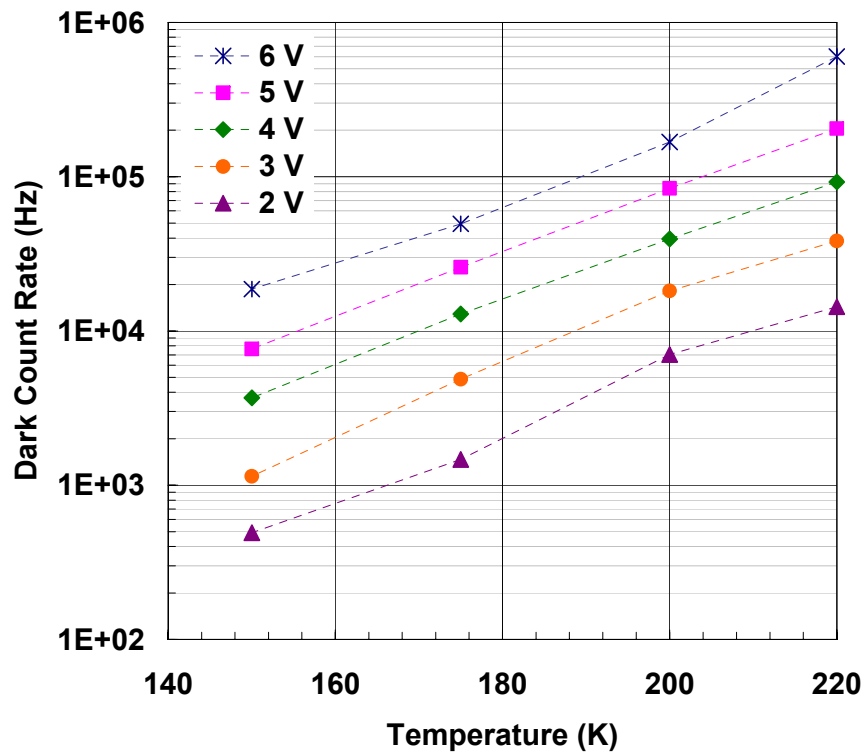
- Dark carriers can be generated by a number of mechanisms



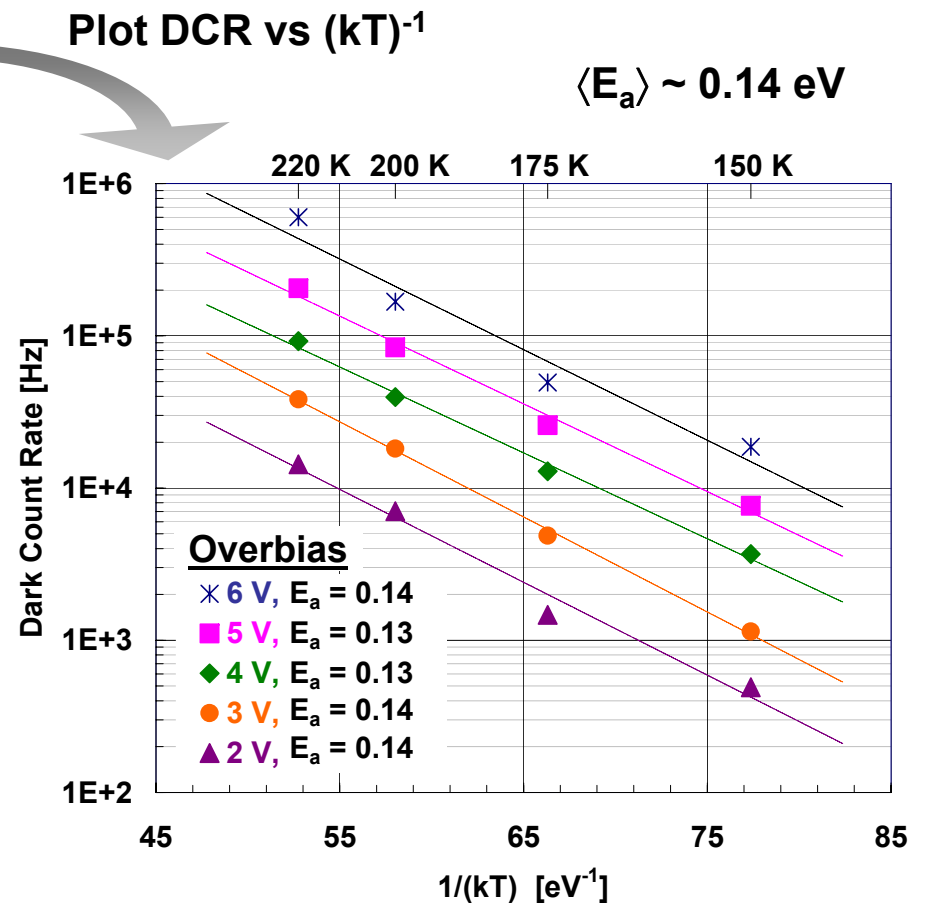
- Sample properties will have a large impact on DCR
 - Bandgap (InP vs. InGaAs vs. InGaAsP)
 - Defects
- Study DCR dependence on temperature and bias for clues
 - **Extract activation energies** to help identify dominant DCR mechanisms

Dark count rate behavior and mechanisms

- Characterize DCR vs. temperature at different overbias for $T < 220$ K
 - Assume $DCR \sim \exp(-E_a/kT)$ to extract activation energy E_a

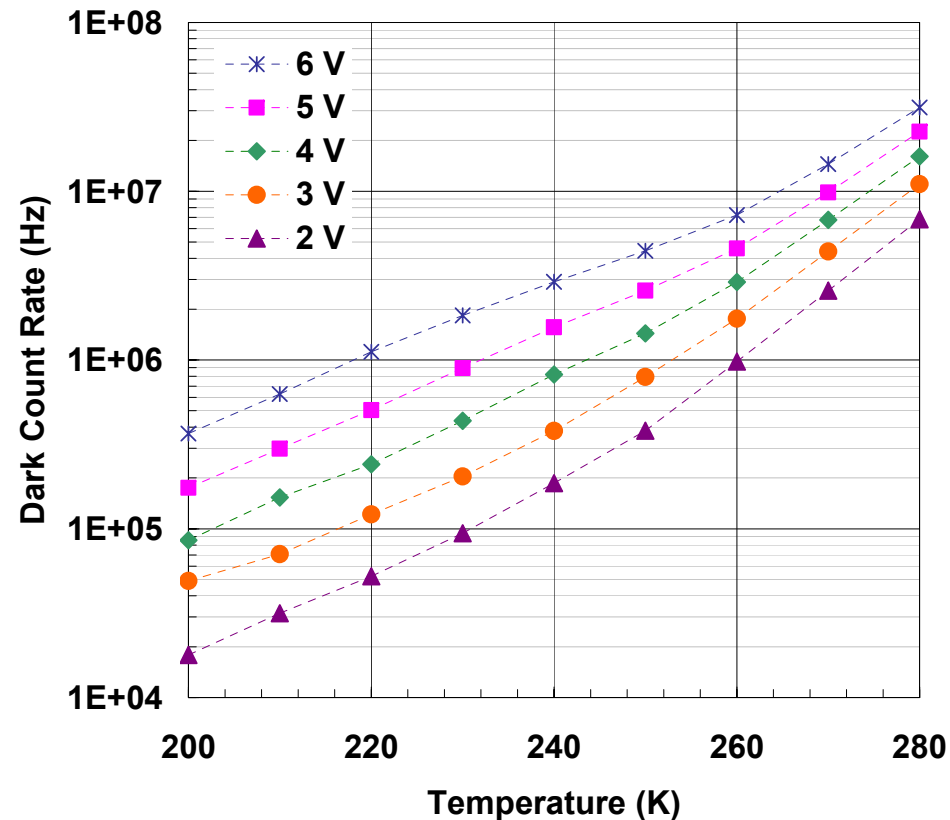


Itzler *et al.*, J. Mod. Opt. 54, p 283 (2007)



Dark count rate behavior and mechanisms

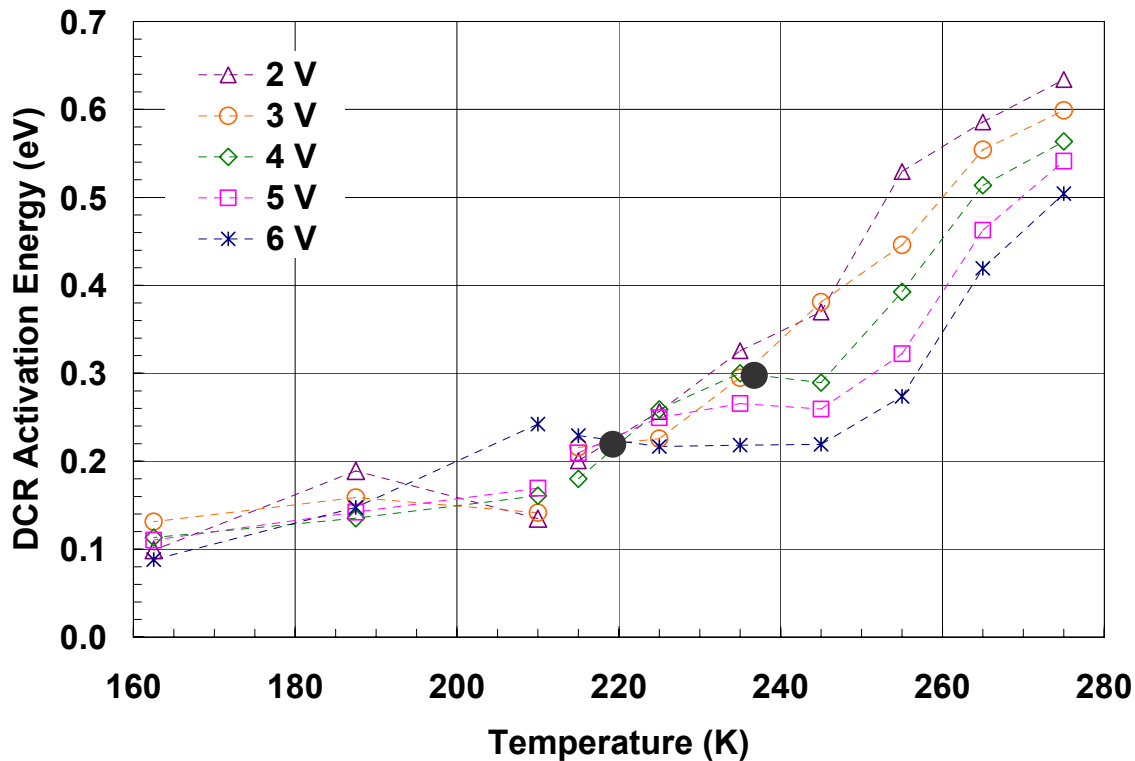
- DCR vs. temperature at different overbias for $T > 200$ K
 - Can not fit with fixed E_a for $T \gtrsim 220$ K



Need to consider $E_a(T)$:
 change in $E_a \rightarrow$ change in dark carrier generation mechanism

Dark count rate behavior and mechanisms

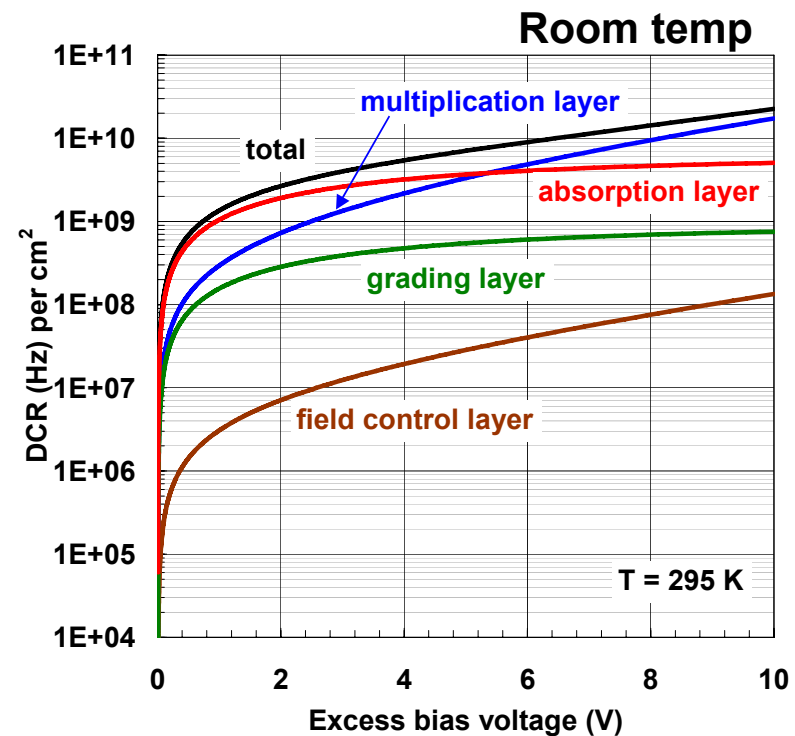
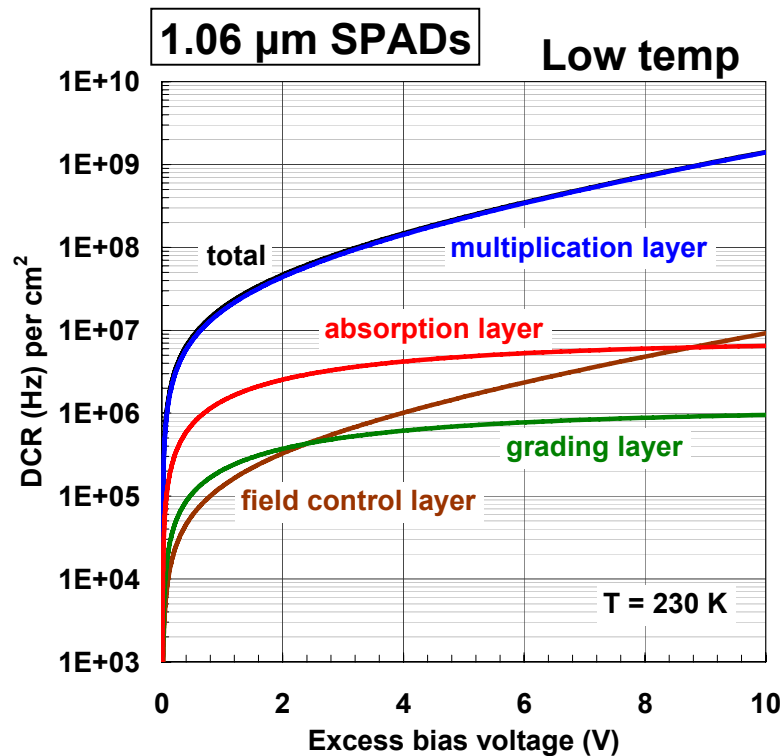
- Consider temperature dependence of DCR activation energy $E_{a,DCR}$



- For $T \lesssim 230$, low $E_{a,DCR}$ → tunneling mechanisms
- For $T \gtrsim 230$, increasing $E_{a,DCR}$ → thermal generation becomes important
 - thermal generation more significant at low overbias

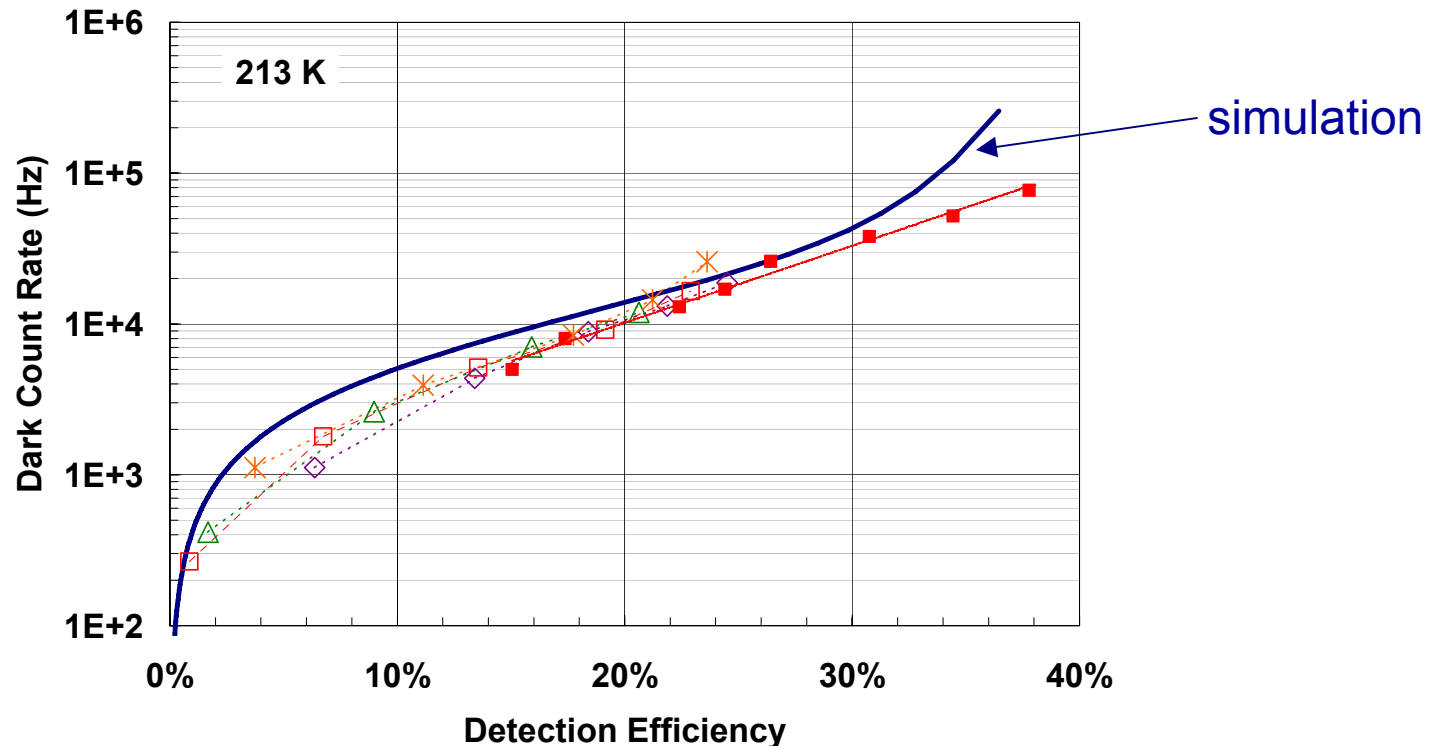
DCR mechanisms for 1.06 μm SPADs

- Simulations give insight into dominant DCR mechanisms
 - following formalism of Donnelly *et al.* [JQE 42, p. 797 (2006)]
- At low temp, multiplication region trap-assisted tunneling dominates
- At room temp, two mechanisms compete
 - absorption region thermal generation dominates at low bias
 - multiplication region trap-assisted tunneling dominates at high bias



Dark count rate modeling for 1.5 μm SPADs

- DCR modeling is more complicated for 1.5 μm SPADs
- First attempts at fitting DCR vs. DE at 1.5 μm are encouraging
 - Fit parameters are similar to those used for 1.06 μm SPADs
 - For 1.5 μm , thermal and tunneling contributions are comparable even at low temp



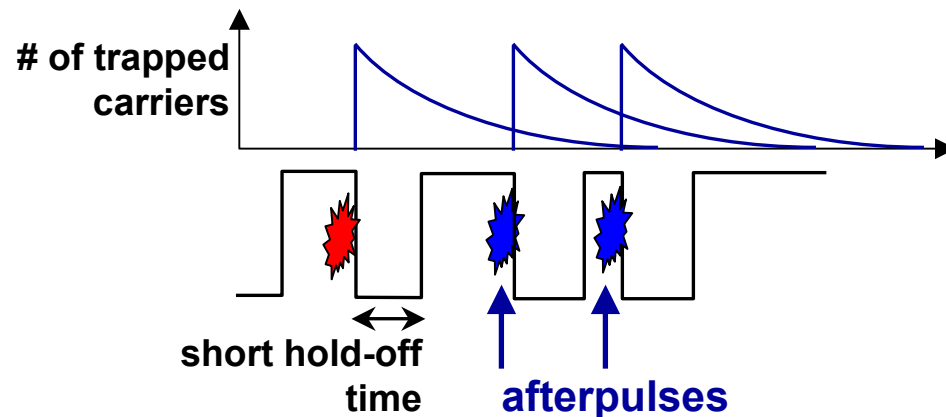
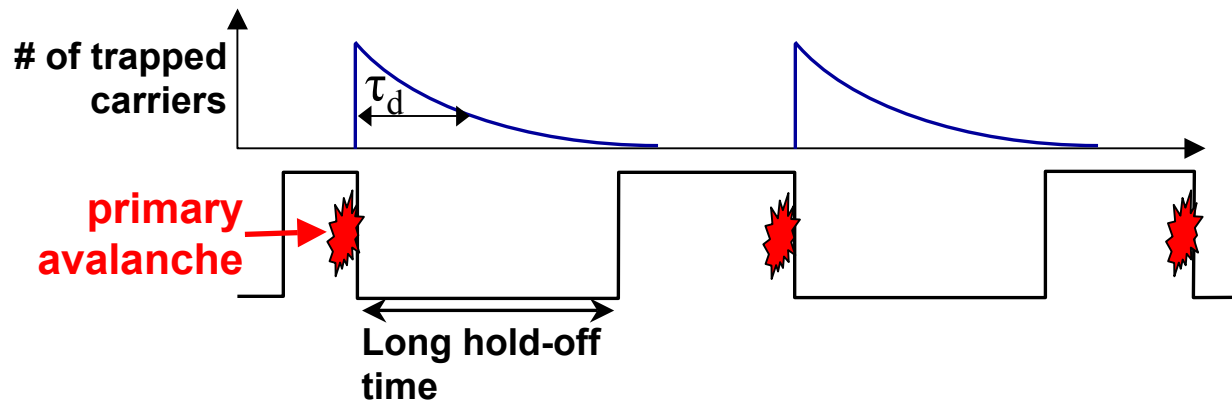
- Simulations very sensitive to defect attributes
- Need appropriate materials analysis (e.g., DLTS/capacitive spectroscopy)

Presentation outline

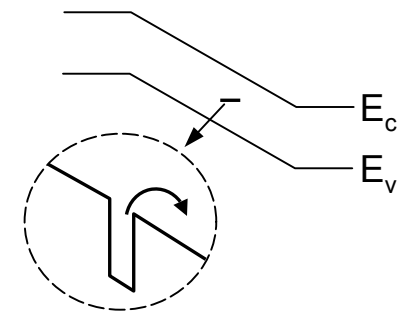
- Motivation for single photon detectors
- Overview of Geiger-mode avalanche photodiodes
- Geiger-mode operation
- Present performance and challenges
 - Dark count rate
 - **Afterpulsing effects**
- Conclusions

Description of afterpulsing

- **Afterpulsing is most serious limitation of InP SPADs; limits repetition rate**
- Avalanche carriers temporarily trapped at defects in InP multiplication region
- Carrier de-trapping at later times can initiate “afterpulse” avalanches
 - Afterpulsing likely if “hold-off” times $T_{h-o} \lesssim$ detrapping time τ_d



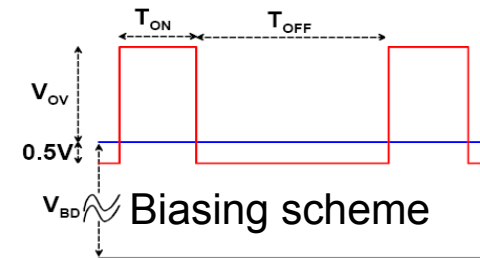
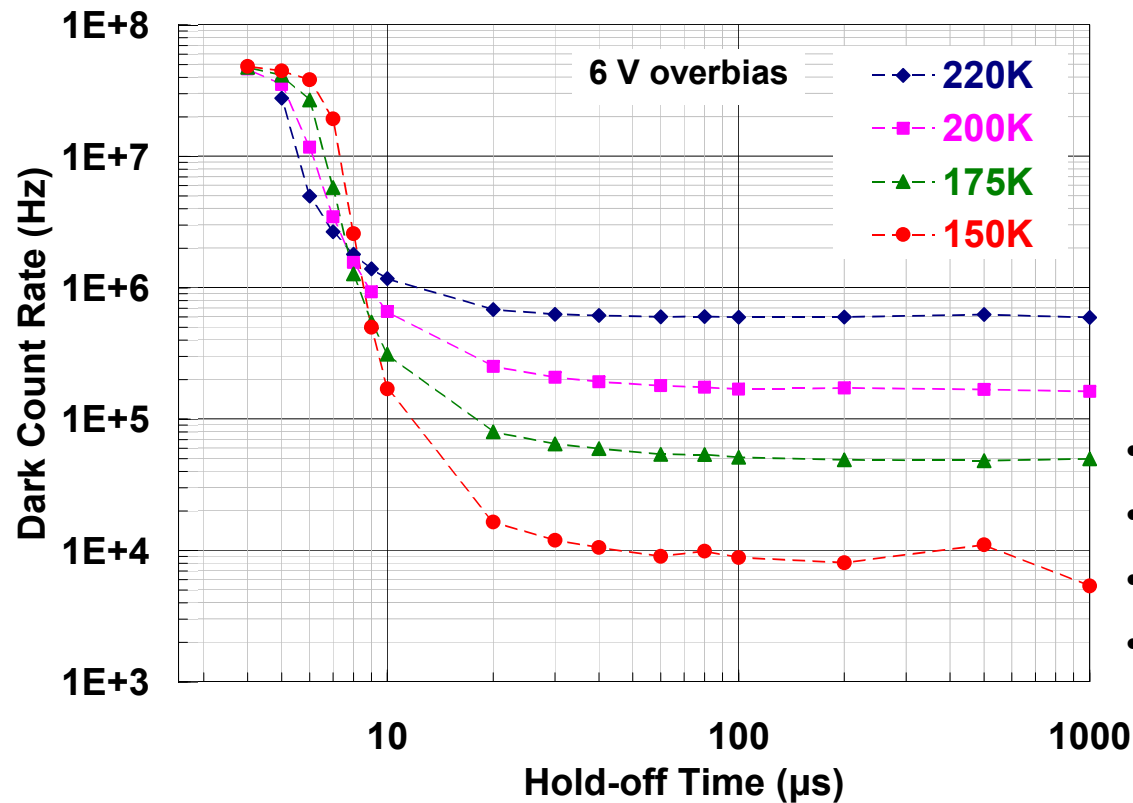
trap sites located in multiplication region



Impact of afterpulsing on count rates

➤ Assess impact of afterpulsing through DCR dependence on hold-off time

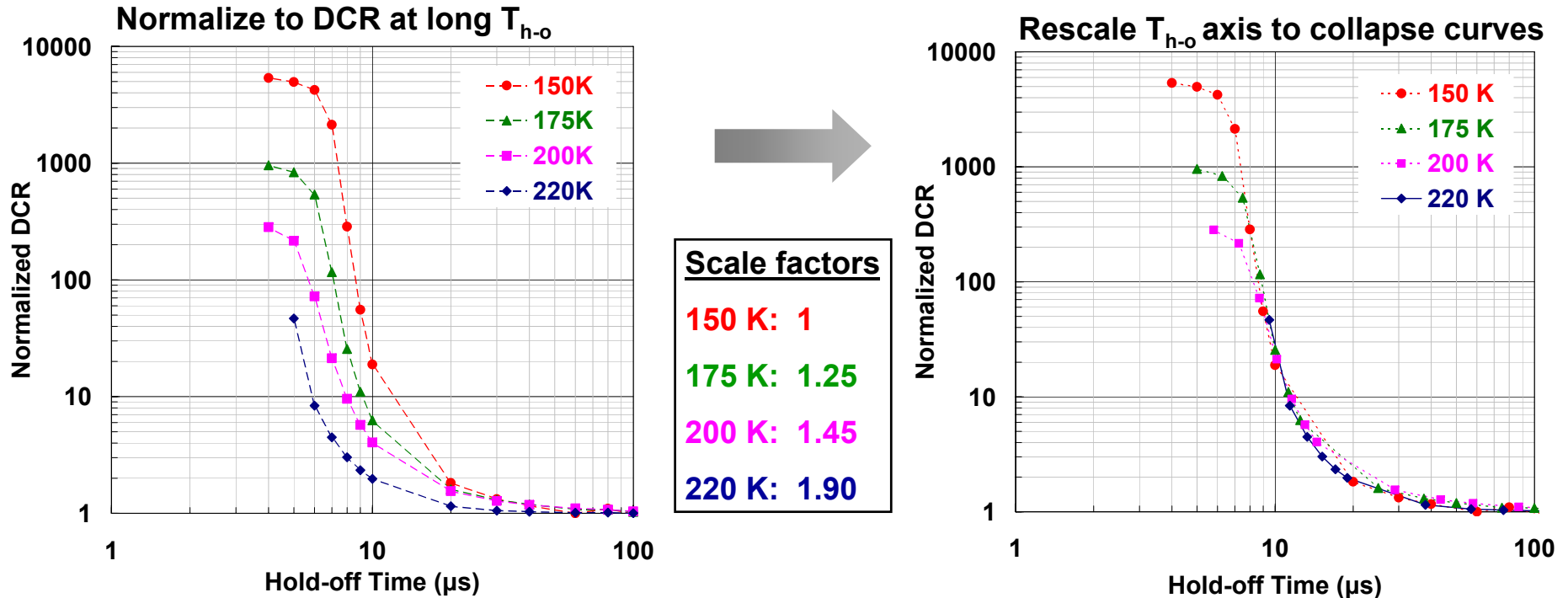
- Looking at afterpulses induced by dark counts only
- Sharp rise in DCR at short T_{h-o} due to afterpulsing



- 40 μm diameter SPADs
- periodic gated operation
- 20 ns gates
- 6 V overbias

Universal scaling of afterpulse behavior

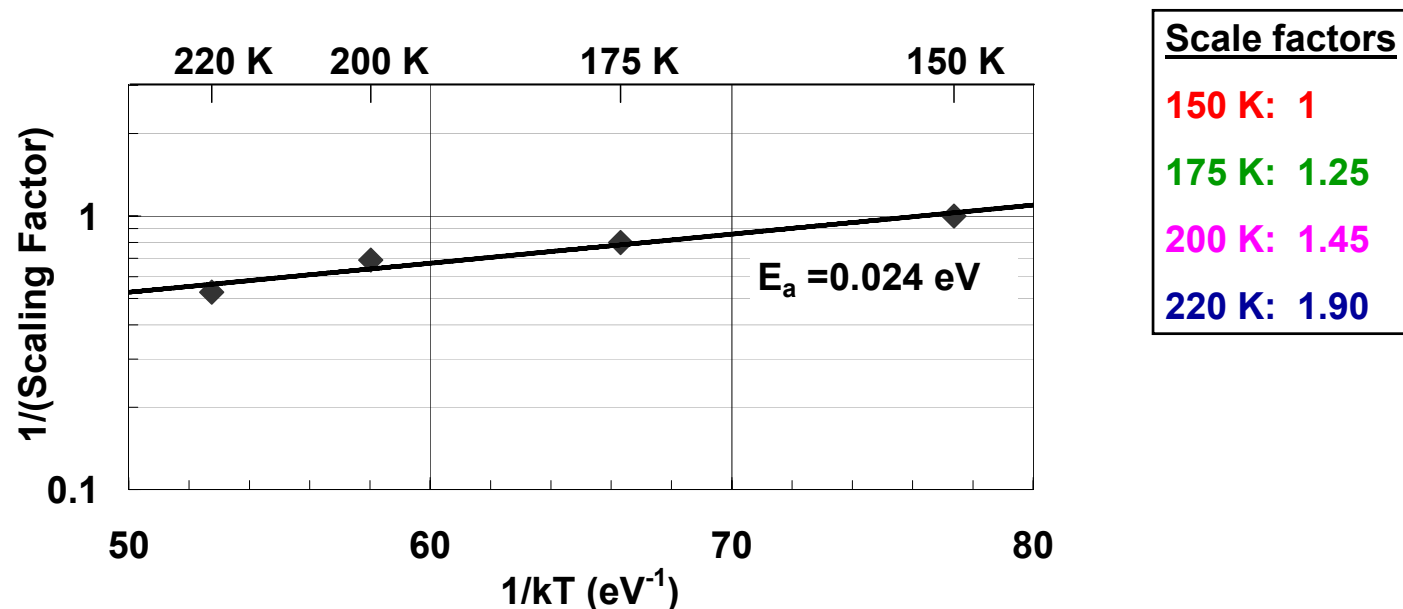
- Normalize to background DCR
- DCR vs. T_{h-o} curves collapse to a single curve with correct rescaling
 - Same curve shape up to temperature-dependence scale factor for T_{h-o}



Collapse allows extraction of afterpulsing activation energy

Afterpulsing activation energy $E_{a,AP}$

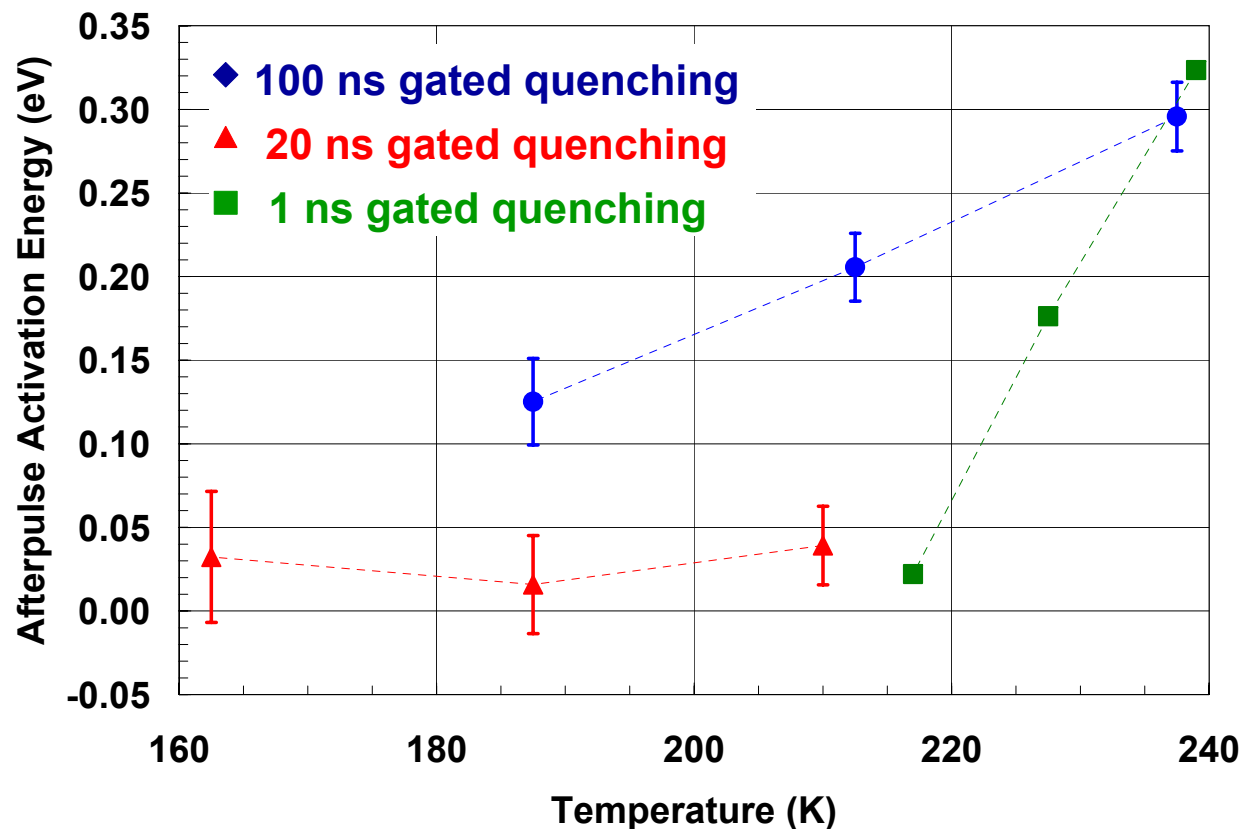
- Use DCR vs T_{h-o} curve collapse to find afterpulse activation energy
 - Assuming single detrapping time τ_d , inverse of scale factor $\propto \tau_d$
 - Plot against $1/kT$ to extract activation energy $E_{a,AP}$



- As with DCR, see if $E_{a,AP}$ depends on temperature
- Consider data from additional measurements

Temperature dependence of $E_{a,AP}$

- **Extract $E_{a,AP}(T)$ to determine trends in afterpulsing behavior**
 - Using very different gate durations, still find consistent trend
 - $E_{a,AP}$ very small ($\lesssim 0.1$ eV) for $T < 200$ K, increases for $T > 220$ K
 - Suggests that scaling may not hold above 220 K – need confirmation



Assume trap lifetime given by:

$$\tau_d = \frac{1}{\sigma v N} \exp\left(-\frac{E_{a,AP}}{kT}\right)$$

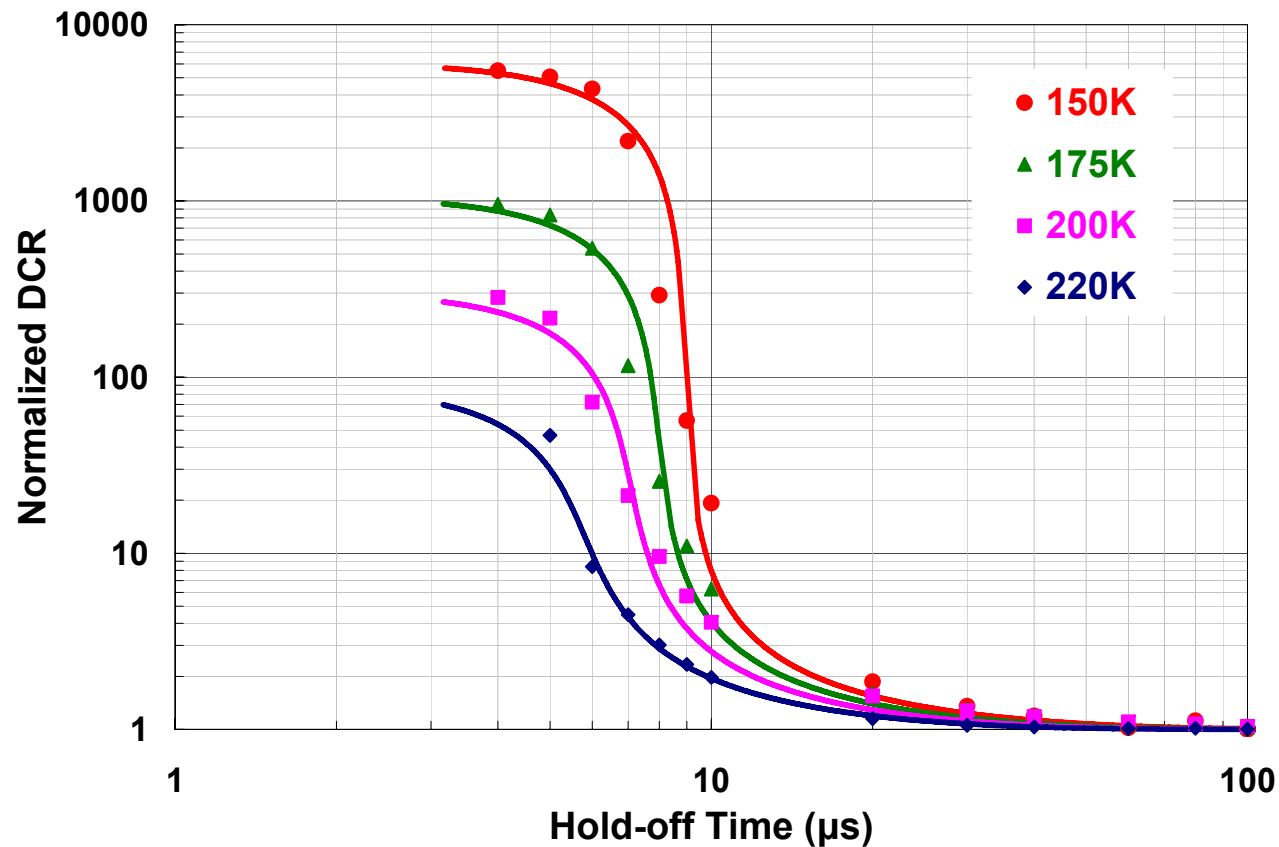
Pre-factor $\propto T^{-2}$

Afterpulsing model fit to gated operation data

➤ Use model of Kang *et al.* to fit measured DCR vs. T_{h-o} data

- Model includes probability of de-trapping from all previous gates
- Initial model assumed single trap; we have added additional traps
- For 220 K, model yields $\tau_d \sim 15 \mu\text{s}$ using single trap

Kang, Lu, Lo,
Bethune, Risk, APL
83, p. 2955 (2003).



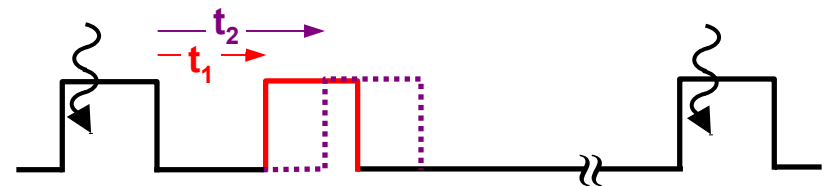
Solid curves:
simulation

Problem of detrapping times

- Recent results related to de-trapping times in InP is quite varied
 - Fundamental question for modeling: single trap vs. multiple traps
 - Multiple traps: too many free parameters, or correct physics?
 - De-trapping times found will depend on range of hold-off times T_{h-o} used
 - For narrow range of T_{h-o} ($< 10X$), see just one de-trapping time from $R_{AP}(t)$

$$R_{AP}(t) = \frac{N_1}{\tau_1} e^{-t/\tau_1} + \frac{N_2}{\tau_2} e^{-t/\tau_2} + \frac{N_3}{\tau_3} e^{-t/\tau_3} + \dots$$

Double-pulse (“pump-probe”) method:



Authors	Temperature [K]	Hold-off time [μs]	Detrapping times [μs]				Technique
			τ_1	τ_2	τ_3	τ_4	
PLI/NASA	250	0.14 – 0.46	0.07				free-running
Jensen <i>et al.</i>	250	1.0 – 10		0.9			double-pulse
Liu <i>et al.</i>	220 – 240	0.02 – 50	0.15	1.0	5	45	double-pulse
Trifonov <i>et al.</i>	195 – 230	1.25 – 100		0.5	6	100	double-pulse
PLI (this work)	200 – 220	4 – 1000			~15	~150	DCR vs. T_{h-o} scaling

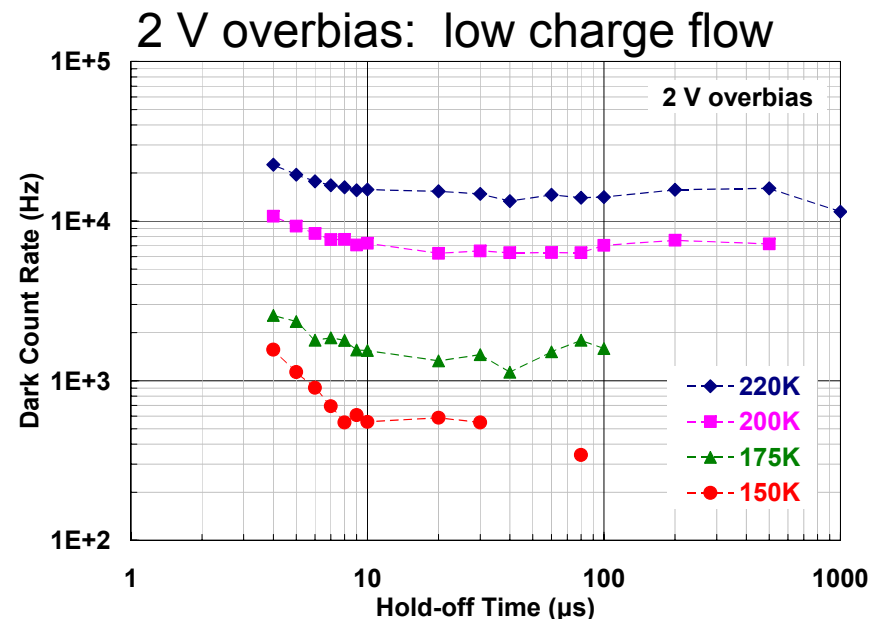
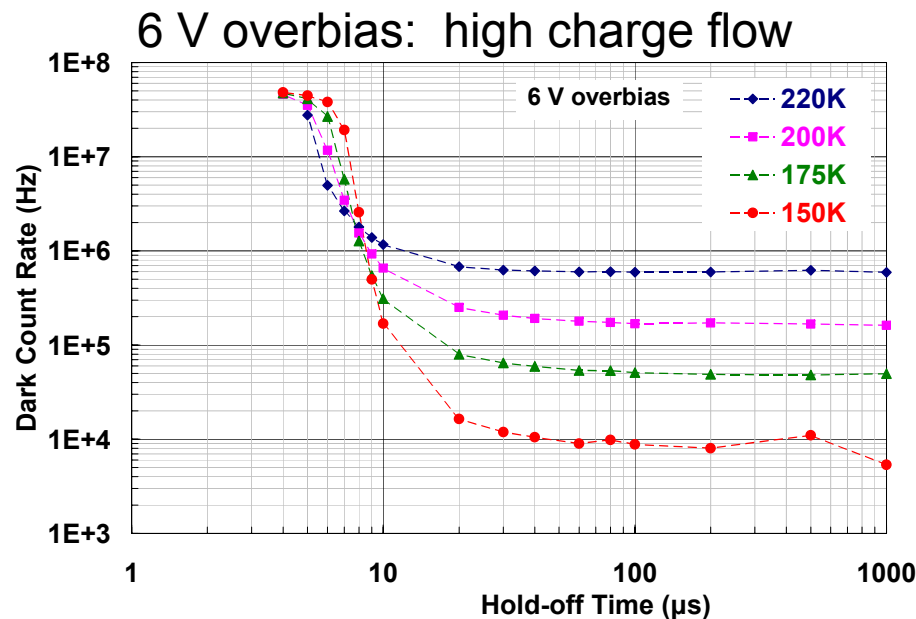
Afterpulsing and Carrier Trapping Mitigation

➤ Impact on afterpulsing from: **materials properties**

- Extract basic properties (trap levels & densities) from measurable quantities (τ_d , E_a)
- Materials improvements are challenging [ref: Si SPAD hold-off times: ~100 ns]

➤ Impact on afterpulsing from: **operating conditions**

- Key factor is total charge flow through device – **reduce charge flow per avalanche**
 - Overbias, quenching conditions, short gates (where possible)
- Higher temperature reduces afterpulsing



Conclusions

- **Present DCR vs. DE: ~10 kHz at 20% at 1.5 μm , $T \sim 215$ K, 25 μm dia.**
- **Temp-dependent DCR activation energy gives insight into mechanisms**
 - Shift from thermal processes at room temperature to tunneling for $T < 220$ K
 - Good simulations should reproduce $E_{a,\text{DCR}}(T)$ behavior
- **Initial simulations provide good description of DCR vs. DE behavior**
 - Valuable for understanding relative contributions of different DCR mechanisms
 - **Need better information regarding defects** and thermal+tunneling mechanisms
- **Afterpulsing is key limitation for high counting rates**
 - Activation energy is constant at low temp, changes at $T > 240$ K
 - Collapse of DCR vs. hold-off time curves indicates universal behavior for $T < 220$
 - **Determination of number of trap types and lifetimes is key** to accurate modeling
 - **Reduce charge flow per avalanche to reduce afterpulsing**